

Clustering in Cooperative Networks

UMass Technical Report TR-UM-CS-2010-67

Boulat A. Bash*, Dennis Goeckel†, Don Towsley*

*Department of Computer Science, University of Massachusetts, Amherst, Massachusetts 01003–9264

†Electrical and Computer Engineering Department, University of Massachusetts, Amherst, Massachusetts 01003–9292

Abstract—Low power ad hoc wireless networks operate in conditions where channels are subject to fading. *Cooperative diversity* mitigates fading in these networks by establishing virtual antenna arrays through clustering the nodes. A cluster in a cooperative diversity network is a collection of nodes that cooperatively transmits a single packet. There are two types of clustering schemes: static and dynamic. In static clustering all nodes start and stop transmission simultaneously, and nodes do not join or leave the cluster while the packet is being transmitted. Dynamic clustering allows a node to join an ongoing cooperative transmission of a packet as soon as the packet is received. In this paper we take a broad view of the cooperative network by examining packet flows, while still faithfully implementing the physical layer at the bit level. We evaluate both clustering schemes analytically as well as using simulations on large multi-flow networks. We demonstrate that dynamically-clustered cooperative networks substantially outperform both statically-clustered cooperative networks and classical point-to-point networks.

I. INTRODUCTION

Low power ad hoc wireless networks typically operate in channel conditions that are subject to time-varying signal degradation known as fading. Diversity mitigates fading by establishing multiple independent channels from source to destination. Unfortunately, radios in extremely low-power ad hoc networks (e.g. sensor networks) use narrow band channels and are unable to employ temporal and frequency diversity. Furthermore, their small size and reliance on batteries have precluded the use of antenna arrays for providing spatial diversity. Thus, *cooperative diversity*, a realization of a multi-antenna array using a *cluster* of single-antenna devices, was proposed as a solution for mitigating fading in ad hoc wireless networks [1]–[3].

A cluster in a cooperative network is a collection of nodes that cooperatively transmits a single packet. There are two types of clustering schemes: static and dynamic. In static clustering [1]–[11] all nodes within a cluster start and stop transmission simultaneously and nodes do not join or leave the cluster while the packet is being transmitted. Dynamic clustering [12]–[15] allows a node to join an ongoing cooperative transmission of a packet as soon as the packet is received. Until now, a comparison of these clustering schemes has not been made. In this work we show that, while the capacity of statically-clustered cooperative networks in our multi-flow scenario is at least double of the capacity of the classical point-to-point networks (i.e. isolated nodes communicating via point-to-point links), using dynamically-clustered cooperation results in the capacity of more than quadruple of the capacity of the point-to-point networks under the same conditions.

Prior to our work, two communities have studied cooperative networks. The fundamental knowledge of the physical layer in wireless networks, including cooperation, comes from the communications community [16], [17]. While dynamic clustering was proposed by this community [12]–[15], most of its work on cooperative diversity focuses on information propagation using static clusters [1]–[6]. Laneman surveys physical layer aspects of cooperation [18]. The networking community generally studies routing multiple packet flows in large statically-clustered cooperative networks [7]–[11]. Kramer et al. [19] provide an exhaustive survey of cooperation, including networking concerns. We have not encountered any previous study of dynamically-clustered cooperation by the networking community.

While previous studies demonstrate the superiority of cooperation over classical point-to-point schemes, a direct performance comparison of the two clustering methods for cooperation is missing and both communities generally have limited evaluation frameworks. Communications research on cooperation is usually conducted in a setting with a single-packet transmission through a network limited to a source, several relays, and a destination. However, networks generally operate with multiple packet flows. While the networks community studies the flows of packets in large networks, the physical layer in its work is often greatly simplified, and we show that such a model can significantly underestimate the capacity achieved by cooperative diversity. Furthermore, previous work has not accounted for interference from other packet transmissions within the same flow. We demonstrate that ignoring such interference can lead to network performance overestimate of as much as a factor of 2.

In this paper we evaluate the performance of the two cooperative diversity clustering methods analytically, and utilize simulations to verify and extend the analysis. The simulations employ multiple flows and hundreds of nodes with the physical layer faithfully implemented at the bit level. Thus, we peer deep into the physical layer, while examining large networks, and are able to accurately compare cooperation schemes under identical channel conditions and energy constraints.

This paper is structured as follows: in the next section we present background on the physical layer. In Section III we describe our system as well as the details of static and dynamic clustering. We present our analytical models of cooperation in Section IV and we analyze the performance of clustering schemes using these models and simulation in Section V. Section VI concludes.

II. WIRELESS COMMUNICATIONS BACKGROUND

In our system, at time t , a complex-valued signal $s_s(t)$ transmitted by sender s is corrupted by an AWGN process $n(t)$ with (two-sided) power spectral density $N_0/2$ and interference from the set \mathcal{I} of interfering transmitters. The channel is subject to path loss and frequency non-selective Rayleigh fading that is independent for different transmitter-receiver pairs. Consequently, the multipath fading gain on a link from a transmitter s to receiver j is a complex zero-mean Gaussian random variable $h_{s,j}$. Thus, the signal $r_{s,j}$ at receiver j is expressed as follows:

$$r_{s,j}(t) = \frac{h_{s,j}(t)s_s(t)}{\sqrt{d_{s,j}^\alpha}} + \sum_{i \in \mathcal{I}} \frac{h_{i,j}(t)s_i(t)}{\sqrt{d_{i,j}^\alpha}} + n(t) \quad (1)$$

where $d_{a,b}$ is the Euclidian distance between nodes a and b and α is the path-loss exponent.

Since fading is a random process, it can be mitigated by using multiple independent channels between transmitter and receiver. This technique is called diversity. We focus on *cooperative diversity*, a technique that utilizes multiple transmitters to establish a virtual antenna array [1]–[3]. With a set of transmitters \mathcal{S} spaced at least a half-wavelength apart, we can establish a cooperative link to the receiver, where the receiver is able to use coordinated, but mutually-independent faded signals from all of the transmitters to decode the message. This is known as a multiple-input single-output (MISO) channel. Diversity in MISO systems is commonly obtained through space-time coding (STC) [17]. Provided that the power of all transmitters in the network is fixed at P_0 and bandwidth is normalized to 1 Hz, the following equation expresses the ergodic capacity of this channel in bits per second (bps) when STC is used [17]:

$$\mathcal{C}(j) = \log_2 \left(1 + \frac{P_0 \sum_{s \in \mathcal{S}} |h_{s,j}|^2 d_{s,j}^{-\alpha}}{N_0 + P_0 \sum_{i \in \mathcal{I}} |h_{i,j}|^2 d_{i,j}^{-\alpha}} \right) \quad (2)$$

For the Rayleigh model, $|h_{a,b}|^2$ is distributed exponentially with mean one. We follow the accepted practice and use (2).

III. SYSTEM DESCRIPTION

A. General Network Framework

We study large ad hoc wireless networks where nodes operate identical half-duplex peak-power limited¹ radios. We are interested in *network capacity*, or the maximum throughput between source and destination that different networks allow under a power constraint, with the throughput normalized by the number of nodes in the network.

The network operates as follows. Each node transmits each packet for b seconds, known as the *transmission period*. The source has an infinite supply of packets, each of size z . The source injects packets into the network by broadcasting a new packet for b seconds and then idling for rb seconds before

¹While we can impose an average power constraint instead, low-power wireless transmitters are often peak power limited, and, in networks dominated by interference (such as the ones we study), the impact of the distinction between average and peak power constraints is minimal. We repeated many of the experiments in this work using an average power constraint and reached similar conclusions.

broadcasting the next packet, where r is termed the *idle-to-busy ratio*. Idling at the source is designed to space out the packets and mitigate intra-flow interference. Parameters b and r control the rate of packet injection into the network.

By (2), node j receives $\mathcal{C}(j)$ bps when the set of nodes \mathcal{S} is transmitting information about the packet desired by j and the set of nodes \mathcal{I} is transmitting different packets. We now discuss two clustering methods enabling cooperative diversity.

B. Statically-clustered Cooperation

Nodes in a static cluster start and stop transmission simultaneously and do not join or leave the cluster while the packet is being transmitted. Statically-clustered cooperation generally outperforms classical point-to-point transmission [7]–[9]. Static clusters alternate between “receive” and “transmit” phases. In its cluster’s receive phase, each node listens to the upstream cluster for the packet. The receive phase ends when the upstream cluster stops transmitting. Then the nodes that received the packet transmit it cooperatively downstream for b seconds.

C. Dynamically-clustered Cooperation

Dynamic clustering relaxes the constraint on when nodes join and leave the actively-transmitting cluster. A node is allowed to join an ongoing cooperative transmission as soon as it receives the packet. Figs. 1 and 2 illustrate an example where a node that is left out of the statically-clustered cooperative transmission is included when dynamic clustering is used.

Dynamic clustering is implemented using mutual information accumulation (MIA). To enable this, the information in the packet is encoded into a set of codewords and transmitted. MIA is the process where the receiver collects codewords until the mutual information of the collected codeword set exceeds the entropy of the packet and it can be decoded. Code combining is used to sum mutual information across symbols [20]. Once the node decodes the packet, it can encode the packet into codewords and join the dynamic cluster by starting transmission. A node transmits each packet for b seconds.

The work that introduced dynamic clustering [15] implemented MIA using a conventional incremental redundancy fixed-rate coding scheme [21]. The drawback of fixed-rate codes is that they may not easily adapt to changes in network conditions and are inefficient when operating outside of their fixed design. Rateless codes [22], [23] have been proposed as a flexible alternative [12]–[14]. However, analysis in [12]–[14] is based on a deterministic channel model and does not account for fading. Furthermore, the analysis in [12]–[15] focused on a single-packet transmission in small networks. Our work is oblivious to the specific implementation of MIA as long as it allows nodes to join cooperative transmission of a packet as soon as the packet is decoded.

We now present the analytical models of cooperation, followed by simulations.

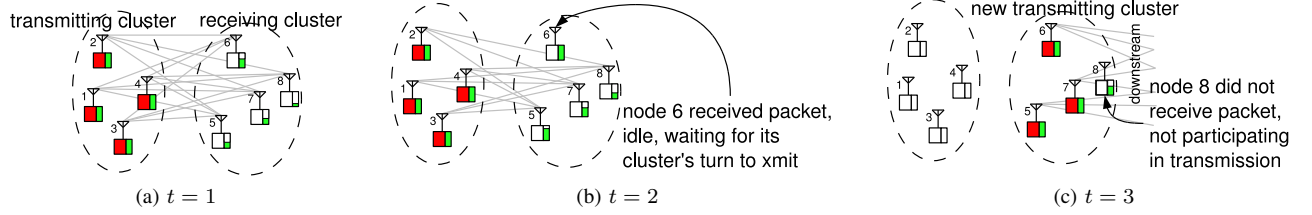


Fig. 1. An example of the evolution of statically-clustered cooperative transmission. See legend in Fig. 3.

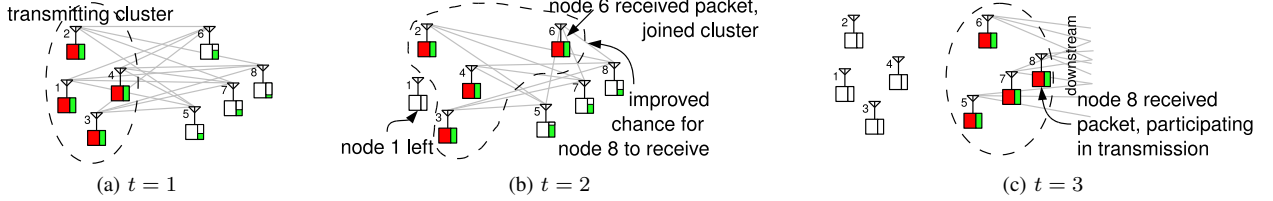


Fig. 2. An example of the evolution of dynamically-clustered cooperative transmission. See legend in Fig. 3.

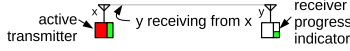


Fig. 3. Legend for Figs. 1 and 2.

IV. ANALYTICAL MODELS OF COOPERATION

In this work we model a flow traversing a strip topology. A strip is a narrow rectangular $l \times w$ 2D lattice of nodes, with one unit of distance separating neighbors along the east-west and north-south axes. Strip topologies are mathematically tractable and have been extensively used in networks research, including literature on cooperative networking [5].

The objective of these models is to approximate the capacity of various configurations of cooperative networks under a power constraint. These models take significantly less computation time than simulation to produce performance estimates and are extendable to multi-flow network scenarios. They are also used to guide parameter selection for simulations that search for actual network capacity. We now discuss models for statically and dynamically clustered cooperation in turn.

A. Statically-Clustered Cooperation

To model statically-clustered cooperation, we define a cluster as a contiguous set of n columns in the strip with nodes labeled 1 through nw according to Figure 4. This labeling scheme is used in all $c = l/n$ identical clusters. Each node is uniquely identified by a tuple (a, u) containing its cluster number a and the label u within the cluster. A statically-clustered cooperative network operates as a time-slotted system; therefore, after each packet is injected into the network by source cluster one, it is received and transmitted in consecutive time slots by clusters 2 through $c - 1$ (in consecutive order) until it is received by the destination in cluster c .

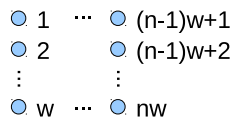


Fig. 4. Node labeling within cluster in the model of static cooperation.

Let $\mathbf{s}_a = (s_{a,1}, s_{a,2}, \dots, s_{a,nw})$ denote the state of each node in cluster a , where $s_{a,u} = 1$ if node u received the packet in the previous time slot from cluster $a - 1$ (and is, therefore, transmitting the packet in the current time slot), and $s_{a,u} = 0$ otherwise. Thus $\mathbf{s}_a \in \{0, 1\}^{nw}$ and a cluster has 2^{nw} states.

Let $\pi(\mathbf{s}_a)$ denote the probability of state \mathbf{s} in cluster a . Let vector $\boldsymbol{\pi}_a \in [0, 1]^{2^{nw}}$ denote the probabilities of all 2^{nw} states of cluster a . We assume that the source node disseminates each packet to its cluster in zero time just before the cluster starts transmitting. (This obviously benefits the statically-clustered network, but is acceptable since we will be using it as a baseline to illustrate the advantages of the dynamically-clustered cooperation.) Therefore,

$$\pi(\mathbf{s}_1) = \begin{cases} 1 & \text{if } \mathbf{s}_1 = \{1\}^{nw} \\ 0 & \text{otherwise} \end{cases}$$

When a is not the source cluster, $a = 2, \dots, c$, a node in a transmits only if it receives the packet from cluster $a - 1$ during the previous time slot. Therefore, the transition probability from state \mathbf{s}_{a-1} to state \mathbf{s}_a is the probability that the nodes transmitting in \mathbf{s}_{a-1} and nodes not transmitting in \mathbf{s}_a do not receive a packet from the nodes transmitting in \mathbf{s}_{a-1} . Denote the set of nodes transmitting in state \mathbf{s}_a as \mathcal{S}_a . To simplify notation, define the bijection $\gamma : \{0, 1\}^{nw} \rightarrow [1, 2, \dots, 2^{nw}]$ and let $j = \gamma(\mathbf{s}_{a-1})$ and $k = \gamma(\mathbf{s}_a)$. Assuming deterministic interference subject only to path loss from the set of transmitters \mathcal{I}_a :

$$P_{jk} = \prod_{r \in \mathcal{S}_a} P \left(z \leq b \log_2 \left(1 + \frac{P_0 \sum_{s \in \mathcal{S}_{a-1}} |h_{s,r}|^2 d_{s,r}^{-\alpha}}{N_0 + P_0 \sum_{i \in \mathcal{I}_a} p_i d_{i,r}^{-\alpha}} \right) \right) \\ \times \prod_{r \notin \mathcal{S}_a} P \left(z > b \log_2 \left(1 + \frac{P_0 \sum_{s \in \mathcal{S}_{a-1}} |h_{s,r}|^2 d_{s,r}^{-\alpha}}{N_0 + P_0 \sum_{i \in \mathcal{I}_a} p_i d_{i,r}^{-\alpha}} \right) \right)$$

where $\sum_{s \in \mathcal{S}_j} |h_{s,r}|^2 d_{s,r}^{-\alpha}$ is a hypoexponential random variable, amenable to numerical analysis, and p_i is the probability that interfering node i is transmitting. This allows us to generate a $2^{nw} \times 2^{nw}$ transition probability matrix $M_{a-1,a}$ for each cluster

$a \in \{2, \dots, c\}$ (there is no transition out of the destination cluster c) and compute state probability vector π_a for cluster a as follows:

$$\pi_a = \pi_1 \prod_{x=2}^a M_{x-1,x}$$

The transition probability matrix varies from cluster to cluster, as the active set of nodes in clusters (and, with it, interference) tends to decrease downstream. Suppose the ID of the interfering node $i \in \mathcal{I}_x$ is (y, u) . We approximate transmission probability p_i of this node as follows:

$$p_i = \sum_{\mathbf{s}_y \text{ s.t. } s_{y,u}=1} \pi(\mathbf{s}_y) \quad (3)$$

For upstream cluster $y < x$, we would have computed π_y prior to π_x . For downstream cluster $y > x$, we approximate by letting $y = x - 1$ and computing an upper bound for p_i using π_{x-1} in place of π_y in (3). This method allows us to compute the destination cluster state probability vector π_c and the corresponding probability of a packet reaching the destination p_d in one pass through the c clusters in the network. Once p_d is computed, the network throughput in bps is:

$$\mathcal{T} = \frac{zp_d}{(1+r)b}$$

We determine an approximation for the network capacity for a given width w , transmitter power constraint P_0 , and packet size z by searching for busy time b^* and corresponding r^* that maximizes \mathcal{T} . We present the results of the numerical evaluation of this model in Section V.

B. Dynamically-clustered Cooperation

To model the dynamically-clustered cooperative network, we assume that the strip divides into groups of $(n+m)$ columns each. Within each group, the upstream n consecutive columns are actively transmitting a packet, while the downstream m consecutive columns are receiving this packet. Active transmitters in one group interfere with transmission of another group. Assuming identical transmitters, the steady state throughput of this network is the throughput of a single group. Thus, in our model, we isolate a $(n+m)$ column group and treat all other transmitters in the network as interferers.

Unlike the dynamic cooperation described in Section III-C, in this model we assume that each packet moves in lockstep through the columns from left to right. That is, nodes join and leave the transmitting cluster in columns, as opposed to individually. Since the numbers of columns transmitting and receiving each packet is always, respectively, n and m , once a column of nodes finishes transmission of the packet and drops out of the cluster, it is immediately replaced by the column that just received the packet.

Since each node transmits a packet for b seconds, the packet moves forward by one column every b/n seconds. Thus, it takes a node mb/n seconds to receive a packet and the total time a node spends on each packet is $mb/n + b = (m+n)b/n$ seconds. Therefore, the idle-to-busy ratio is $r = m/n$. For an

end-to-end packet loss rate of p_l , network throughput, in bits per second, is then

$$\mathcal{T} = \frac{nz(1-p_l)}{(n+m)b} \quad (4)$$

Our model contains two components: one to compute the idle-to-busy ratio r , and the other to determine the end-to-end packet loss probability p_l . We describe each component in turn and show how they can be used to approximate the capacity of dynamically-clustered cooperative network.

1) *Idle-to-Busy Ratio*: We know that after every b/n seconds the packet must move forward by one column. We assume a completely deterministic channel model without fading, subject only to path-loss. Then, node j receives the following amount of information (in bits) during the b/n seconds it is x columns away from the front of the sending group:

$$q_j(x) = \frac{b}{n} \log_2 \left(1 + \frac{P_0 \sum_{s \in \mathcal{S}_x(j)} d_{s,j}^{-\alpha}}{N_0 + P_0 \sum_{i \in \mathcal{I}_x(j)} (1-p_l) d_{i,j}^{-\alpha}} \right) \quad (5)$$

where $\mathcal{S}_x(j)$ denotes the set of nodes that are actively sending the packet to j while j is x columns away from the front of the receiving group and $\mathcal{I}_x(j)$ denotes the set of nodes interfering with the transmission to j . Thus, the sum in the numerator is the total signal received by j from the n columns that are transmitting the packet; and the sum in the denominator is the total interference adjusted by the packet loss probability.

In order for the packet to progress, each node j must receive all z bits of each packet within its allotted time mb/n , which means that the following must be satisfied:

$$z \leq \sum_{x=0}^{m-1} q_j(x) \quad (6)$$

2) *End-to-End Loss Rate*: We approximate end-to-end packet loss rate p_l by the loss rate of the first hop from the source node. Our premise is that once some node decodes a copy of the packet and forms a cluster with the source, other nodes acquire enough information from this two-node cluster to finish decoding the packet and are able to join the cluster themselves. However, if this initial two-node cluster does not form, the packet is lost. Since the source waits for mb/n seconds between packet transmissions, the initial receiving set of nodes \mathcal{R} contains the nodes in the first m columns of the strip, including receivers in the column containing the source. The probability that a packet is lost by \mathcal{R} is:

$$p_l = \prod_{r \in \mathcal{R}} p_l(r)$$

where $p_l(r)$ is the probability that r did not receive the packet.

We assume Rayleigh fading between the source and each receiver in \mathcal{R} . However, we assume no fading, just path loss, between the source and the interfering nodes. Then, since

$|h_{s,r}|^2$ is exponentially distributed with mean one:

$$\begin{aligned} p_l(r) &= P\left(z > b \log_2 \left(1 + \frac{P_0 |h_{s,r}|^2 d_{s,r}^{-\alpha}}{N_0 + P_0 \sum_{i \in \mathcal{I}} d_{i,r}^{-\alpha}}\right)\right) \\ &= 1 - \exp\left(-\frac{(2^{z/b} - 1)(N_0 + P_0 \sum_{i \in \mathcal{I}} d_{i,r}^{-\alpha})}{d_{s,r}^{-\alpha} P_0}\right) \end{aligned}$$

where \mathcal{I} denotes the interfering set of transmitters.

3) *Using the model:* Given network width w , transmitter power constraint P_0 , packet size z , transmitter busy time b and values of m and n , we can easily compute p_l . Thus, through manipulating m , n , and b we can find approximate capacity by maximizing (4) subject to constraint (6).

V. EXPERIMENTAL RESULTS

In this section we present numerical results obtained from the analytical models described in Section IV as well as results from simulations. We start by describing our experimental setup. We then motivate our bit level simulations of cooperative networks and present the comparison between cooperative clustering schemes in single and multiple flow settings.

A. Simulation Setup

We use MATLAB to evaluate our analytical models and we developed a network simulator in C that implements the physical layer on the bit level using a block Rayleigh fading channel model. Analytical results shown on Figs. 7, 11 and 12 took several hours of computation time on a quad-core Core2 machine, while the simulation results on the same figures took about a week to compute on a cluster with 400 Xeon cores. Most of our experiments are based on strip network topologies defined in Section IV (we assess the impact of randomizing the network topologies in Section V-D). Our approach allows us to compare the performance of the clustering schemes independent of routing. In a more realistic setting, we envision a routing protocol connecting the source and the destination that would include a mechanism to ensure cooperation of the nodes along the path (similar to braided routing [24]).

We fix the strip length at $l = 100$ nodes and vary the width w . Thus our networks have hundreds of nodes,² like prior simulation studies [7]–[9]. For statically-clustered cooperation, we report results for single-column clusters since they outperform other arrangements. The source and destination are at opposite ends of the strip. In statically-clustered cooperation the source node disseminates each packet to its cluster in zero time just before the cluster starts to transmit. The packet length is $z = 500$ bits, and $\alpha = 4$ is the path-loss exponent.³

Each transmitter has peak power P_0 ; for a given signal-to-noise ratio P_0/N_0 , we adopt the standard convention of letting $N_0 = 1$ and vary P_0 . We compute network capacity for values of P_0 between 10 dB and 20 dB and various strip widths w by maximizing the throughput over the transmission period b and

²We experimented with network lengths as short as $l = 20$ and observed similar results.

³We experimented with $\alpha = 3$ and obtained similar results (see Fig. 6).

source idle-to-busy ratio r . We report total network capacity divided by strip width w to match the normalization of the multiple flow case. Each simulation is run for 10^6 seconds to ensure that network performance reaches steady state.

B. Limitations of Previous Cooperative Diversity Analysis

To motivate the bit level simulation of cooperative networks, we present two limitations of previous cooperation studies.

1) *Cluster modeled as a single node with multi-antenna array:* In [7], [8] the authors use an off-the-shelf simulator to model a statically-clustered cooperative diversity network of randomly located nodes with 4-node clusters. Since cooperative diversity is not directly supported by the simulator, one node per cluster actually transmits the packet with an additional power gain of $D = 15$ dB (spatial diversity gain from using 4 antennas at bit error rate of 10^{-3} [16]); other cluster members are idle. We call this method of using uniform diversity gain to model static clusters the *power boost approximation* (PBA). Because PBA fixes the diversity order of every transmission to be equal, we would expect it to be most accurate in regular (as opposed to random) topologies. Here we apply PBA in our structured networks. We estimate the capacities of two statically-clustered single-flow networks with clusters containing two and four nodes ($w = 2$ and $w = 4$) using PBA, and compare with the capacities obtained via full simulation of the corresponding networks on Fig. 5. The PBA curves represent the capacities of point-to-point networks where all transmitters are operating at D dB above the peak power of the corresponding cooperative networks, with $D = 10$ dB for PBA of the network with 2-node clusters and $D = 15$ dB for 4-node clusters. PBA capacities are normalized by the cluster sizes of the corresponding networks. Fig. 5 shows that PBA significantly underestimates the capacity as the transmitter power increases.

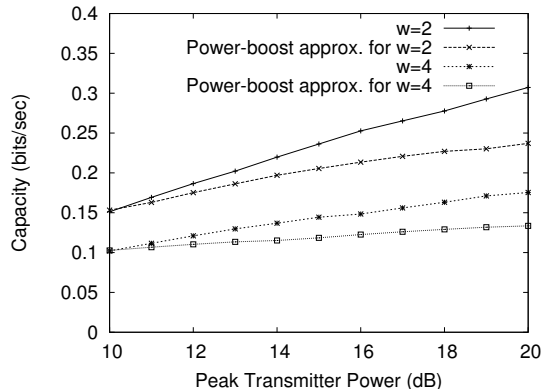


Fig. 5. Capacities of statically-clustered single-flow networks vs. PBA.

2) *Ignoring interference:* Fig. 6 shows the effect of ignoring intra-flow interference on the capacities of two single-flow dynamically-clustered cooperative networks of width $w = 2$ with path-loss exponents $\alpha = 3$ and $\alpha = 4$. As expected, omitting interference results in a substantial overestimate of capacity. The figure also shows that the small difference in path-loss exponent α does not result in significant capacity changes.

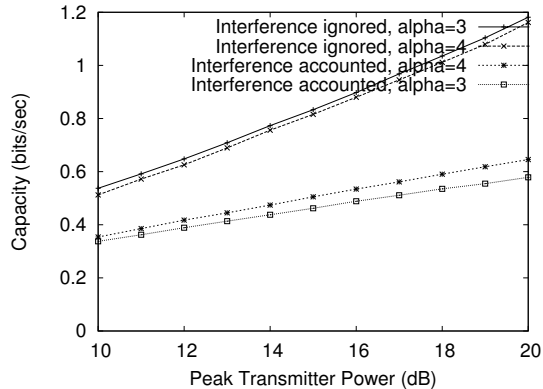


Fig. 6. Omission of interference (dynamic clusters, $w = 2$)

C. Comparison of Clustering Schemes on Single-flow Networks

We evaluate the normalized network capacities of statically and dynamically-clustered single-flow networks for strip widths $w = \{1, 2, 3, 4\}$ and report the results in Fig. 7. The analytical models agree with simulation, and, as shown on Fig. 8, both models are reasonably accurate at approximating the parameters b and r that lead to operation at network capacity.

The reason for the substantial gain from using dynamic clustering is its opportunistic approach to utilizing network resources. A node in the dynamically-clustered network joins the cluster by starting packet transmission as soon as it receives the packet. This node is usually on the frontier of the cluster, and has a better channel (on average) to nodes that have not yet received the packet. By the time that node stops transmitting, the frontier has moved on, and the node is no longer needed to move that packet downstream. Smaller idle-to-busy ratios r in dynamic networks (shown on Fig. 8) illustrate that the dynamic clusters are faster and tighter-packed than static. In our experiments the best dynamically-clustered network, while employing half as many nodes, delivered 40% more packets than the best statically-clustered network.

D. Impact of Randomized Topologies

Since most deployed wireless networks are not as regular as a strip, we examine the sensitivity of our results to randomness. Fig. 9 shows the capacity of dynamically-clustered cooperation on *randomized strip* topologies. These topologies are constructed by dividing a $w \times l$ rectangle into wl unit squares, and placing one node in a random location within each square. Though topological randomness degrades network performance, it does not change our general results, since dynamically-clustered cooperation on a randomized topology outperforms statically-clustered cooperation on a regular strip.

E. Impact of Multiple Flows

Finally, we examine multiflow cooperative networks. We consider a grid of identical nodes with flows traversing the grid vertically and horizontally in either direction, as illustrated in Fig. 10. Such a grid can be embedded in a network of randomly placed nodes [25]. We are interested in the per flow capacity of a grid network with flows traveling horizontally left to right

(highlighted flows in Fig. 10), since TDMA can divide this capacity among flows running in both directions vertically and horizontally [26]. Thus, we simulate flows on parallel strips of length $l = 100$ nodes at least one unit distance apart. We report the total capacity per flow divided by the number of rows w used by the flow plus s additional units distance separating each flow from the neighboring flow, normalizing the capacity by the *area* the flows occupy. The parameters b and r are the same for all flows. We assume that the adjacent sources synchronize their transmissions and inject packets $(1+r)b/2$ seconds apart, thus alternating phases of their busy cycles. This is reasonable since it takes a source $(1+r)b$ seconds to detect its neighbor's busy cycle. We thus reduce interference without sacrificing network capacity and produce a checkerboard flow pattern in Fig. 10.

Figs. 11 and 12 report the per flow capacity for statically and dynamically-clustered multiflow networks. The analytical models described in Section IV are extended by accounting for interference from additional flows. The extended analytical models agree with the multiflow simulation, and, as shown on Fig. 13, are reasonably accurate at approximating the parameters b and r that lead to operation at network capacity.

As in single-flow networks, dynamic clustering outperforms static clustering. Neither clustering scheme requires additional separation ($s = 0$) between the flows to maximize the capacity. For static clustering, two-node clusters ($w = 2, s = 0$) maximize capacity, as in the single-flow case. For dynamic clustering, two-node wide strips ($w = 2, s = 0$) maximize the capacity. The increase in strip width over the single-flow scenario is sensible, since a narrow cooperative cluster is more vulnerable to interference from the other flows.

VI. CONCLUSION

The objective of this work is to directly compare the two clustering methods for cooperative networks. Our main contribution is the demonstration of substantial performance gain from using dynamic instead of static clustering in large cooperative networks. We also show the importance of accounting for the intra-flow interference. Finally, we provide comprehensive evaluation of the cooperative network performance. Our analytical models quickly determine reasonable network capacity estimates while the simulation engine both accurately implements the physical layer at the bit level and supports large multiple-flow networks. In the future we would like to develop scalable protocols to deal with changing workload conditions in cooperative networks.

REFERENCES

- [1] J. N. Laneman, "Cooperative diversity in wireless networks: Algorithms and architectures," Ph.D. dissertation, Massachusetts Institute of Technology, 2002.
- [2] A. Sendonaris, E. Erkip, and B. Aazhang, "User cooperation diversity. part I. system description," *IEEE Transactions on Communications*, vol. 51, no. 11, pp. 1927–1938, Nov. 2003.
- [3] —, "User cooperation diversity. part II. implementation aspects and performance analysis," *IEEE Transactions on Communications*, vol. 51, no. 11, pp. 1939–1948, Nov. 2003.

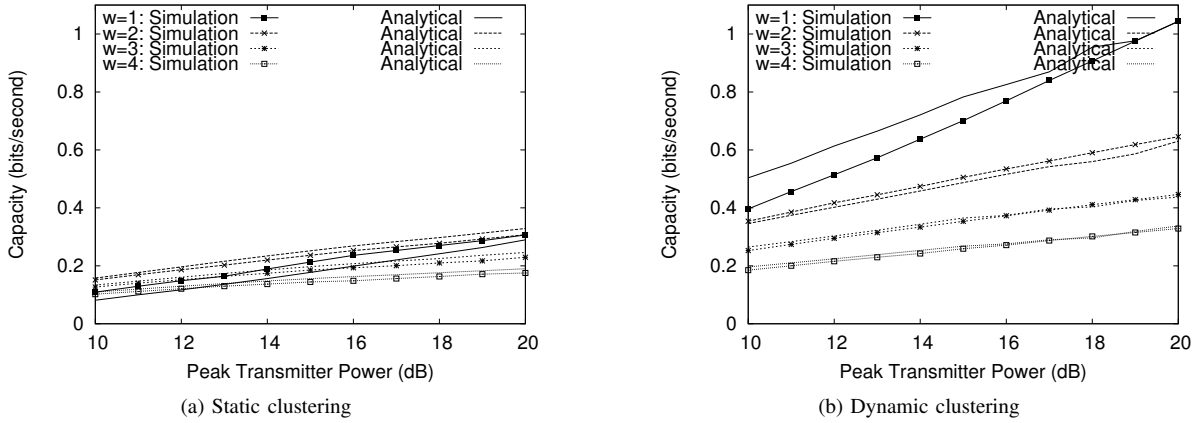


Fig. 7. Analytical and simulated performance of single-flow cooperative networks for different strip widths w .

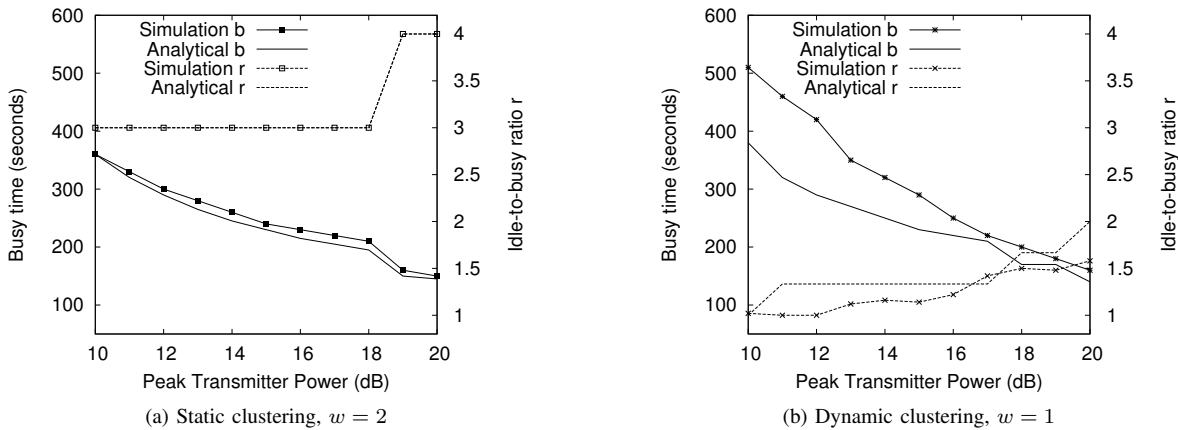


Fig. 8. Parameters that yield maximum capacity in the simulation and the model of the single-flow cooperative networks. Busy time b is plotted on the left y -axis, idle-to-busy ratio r on the right y -axis.

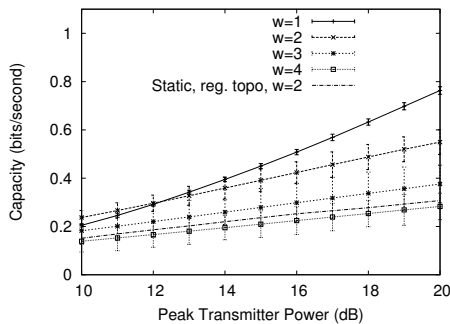


Fig. 9. Performance of dynamically-clustered cooperation on randomized strip topologies (with best-performing instance of statically-clustered cooperation on regular strip network given.) The results for dynamically-clustered scheme were obtained by averaging the single-flow performance on 30 randomly-generated topologies. 5% confidence intervals are reported.

- [4] L. V. Thanayankizil, A. Kailas, and M. A. Ingram, "Routing protocols for wireless sensor networks that have an opportunistic large array (OLA) physical layer," *Ad Hoc and Sensor Wireless Networks, Special Issue on Sensor Technologies and Applications*, vol. 8, no. 1–2, pp. 79–117, 2009.
- [5] A. Kailas and M. Ingram, "Analysis of a simple recruiting method for cooperative routes and strip networks," *IEEE Transactions on Wireless Communications*, no. 99, pp. 1–5, Jul. 2010.
- [6] A. Scaglione, D. L. Goeckel, and J. N. Laneman, "Cooperative communications in mobile ad hoc networks," *IEEE Signal Processing Magazine*,

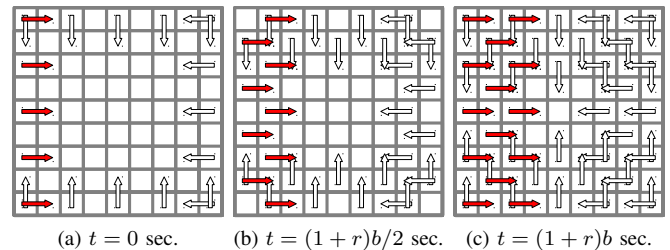


Fig. 10. Flows on the grid. We compute the capacity of the highlighted flows.

- vol. 23, no. 5, pp. 18–29, Sep. 2006.
- [7] G. Jakllari, S. V. Krishnamurthy, M. Faloutsos, and P. V. Krishnamurthy, "On broadcasting with cooperative diversity in multi-hop wireless networks," *IEEE Journal on Selected Areas in Communications*, vol. 25, no. 2, pp. 484–496, Feb. 2007.
- [8] G. Jakllari, S. V. Krishnamurthy, M. Faloutsos, P. V. Krishnamurthy, and O. Ercetin, "A cross-layer framework for exploiting virtual MISO links in mobile ad hoc networks," *IEEE Transactions on Mobile Computing*, vol. 6, no. 6, pp. 579–594, Jun. 2007.
- [9] S. Lakshmanan and R. Sivakumar, "Diversity routing for multi-hop wireless networks with cooperative transmissions," in *Proc. of SECON*, Rome, 2009.
- [10] S. Sharma, Y. Shi, Y. T. Hou, H. D. Sherali, and S. Kompella, "Cooper-

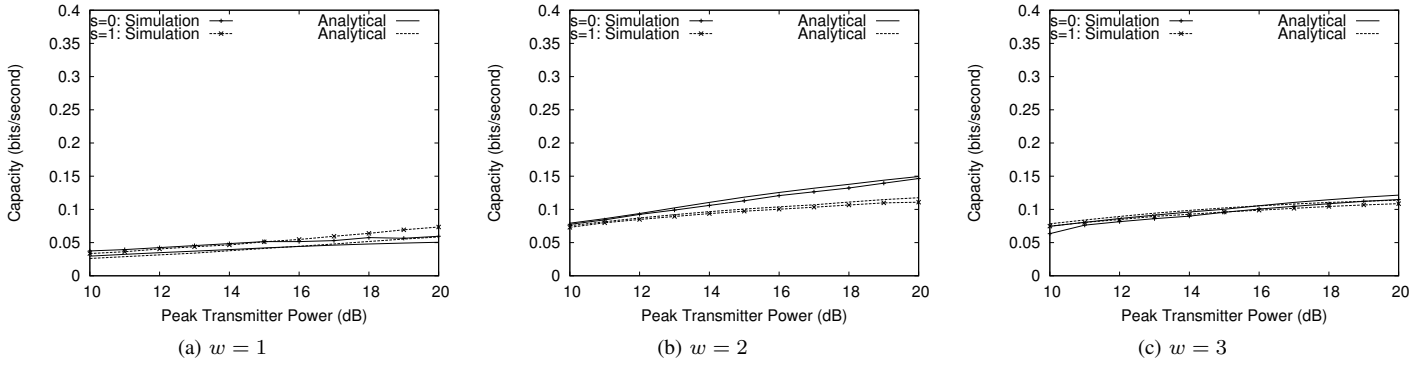


Fig. 11. Analytical and simulated performance of multi-flow statically-clustered cooperative networks for varying strip width w and inter-flow separation s .

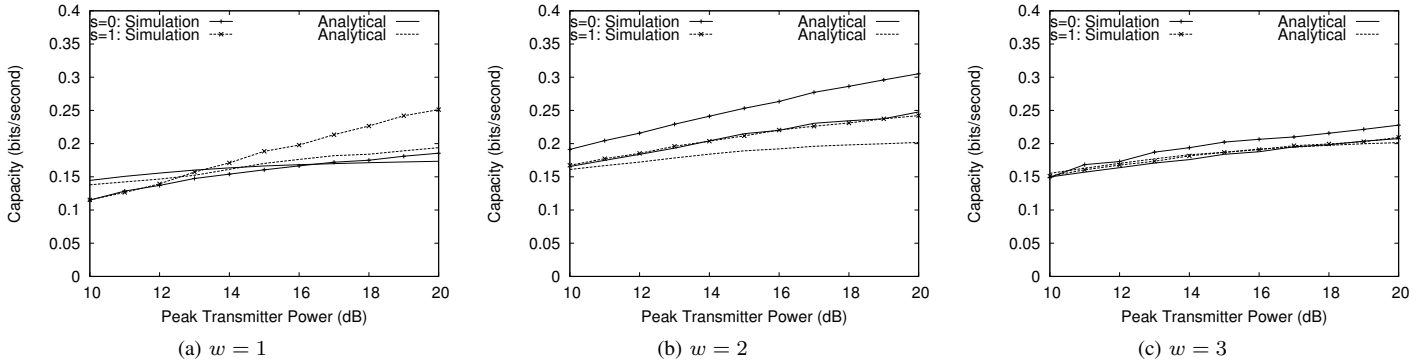


Fig. 12. Analytical and simulated performance of multi-flow dynamically-clustered cooperative networks for varying strip width w and inter-flow separation s .

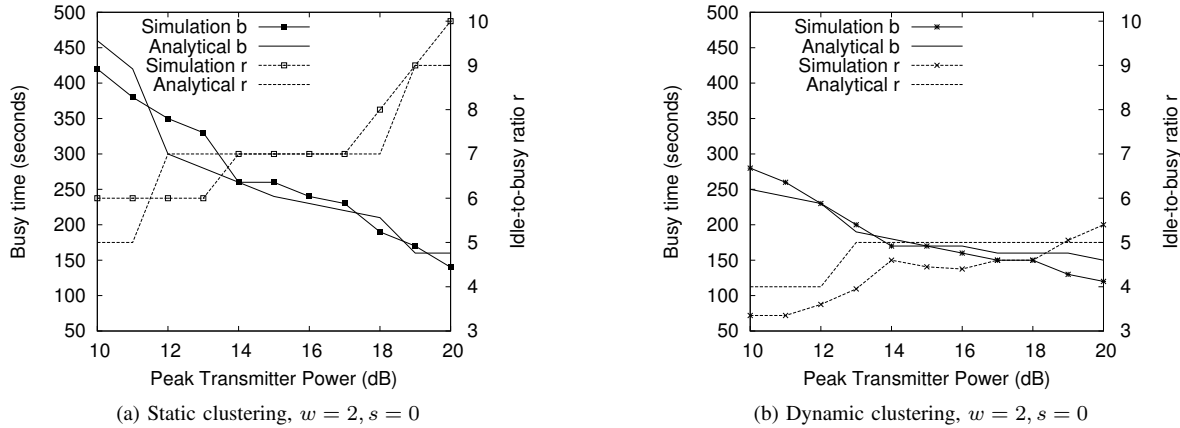


Fig. 13. Parameters that yield maximum capacity in the simulation and the model of the multi-flow cooperative networks. Busy time b is plotted on the left y -axis, idle-to-busy ratio r on the right y -axis.

- ative communications in multi-hop wireless networks: Joint flow routing and relay node assignment,” in *Proc. of INFOCOM*, San Diego, CA, 2010.
- [11] J. Zhang and Q. Zhang, “Cooperative routing in multi-source multi-destination multi-hop wireless networks,” in *Proc. of INFOCOM*, Phoenix, AZ, 2008.
- [12] S. C. Draper, L. Liu, A. F. Molisch, and J. S. Yedidia, “Routing in cooperative wireless networks with mutual-information accumulation,” in *ICC 2008*, May 2008, pp. 4272–4277.
- [13] S. Draper, L. Liu, A. Molisch, and J. Yedidia, “Cooperative routing for wireless networks using mutual-information accumulation,” Mitsubishi Electric Research Laboratories, Tech. Rep. 2009–055, Sep. 2009.
- [14] A. F. Molisch, N. B. Mehta, J. S. Yedidia, and J. Zhang, “Performance of fountain codes in collaborative relay networks,” *IEEE Transactions on Wireless Communications*, vol. 6, no. 11, pp. 4108–4119, Nov. 2007.
- [15] B. Zhao and M. C. Valenti, “Practical relay networks: A generalization of Hybrid-ARQ,” *IEEE Journal on Selected Areas in Communications*, vol. 23, no. 1, pp. 7–18, 2005.
- [16] J. G. Proakis, *Digital Communications*, 4th ed. New York, NY: McGraw Hill, 2000.
- [17] D. Tse and P. Viswanath, *Fundamentals of Wireless Communication*. Cambridge University Press, 2005.
- [18] J. N. Laneman, “Cooperative diversity: Models, algorithms, and architectures,” in *Cooperation in Wireless Networks: Principles and Applications*. Springer, 2006, ch. 1, pp. 163–188.
- [19] G. Kramer, I. Marić, and R. D. Yates, “Cooperative communications,” *Found. Trends Netw.*, vol. 1, no. 3, pp. 271–425, 2006.
- [20] G. Caire and D. Tuninetti, “The throughput of hybrid-ARQ protocols

- for the gaussian collision channel," *IEEE Transactions on Information Theory*, vol. 47, no. 5, pp. 1971–1988, Jul. 2001.
- [21] S. B. Wicker, *Error Control Systems for Digital Communication and Storage*. Prentice Hall, 1995.
- [22] M. Luby, "Lt codes," in *The 43rd Annual IEEE Symposium on Foundations of Computer Science*, 2002, pp. 271–282.
- [23] M. Luby, A. Shokrollahi, M. Watson, and T. Stockhammer, "Raptor Forward Error Correction Scheme for Object Delivery," IETF RFC 5053.
- [24] D. Ganesan, R. Govindan, S. Shenker, and D. Estrin, "Highly-resilient, energy-efficient multipath routing in wireless sensor networks," *SIGMOBILE Mob. Comput. Commun. Rev.*, vol. 5, no. 4, pp. 11–25, 2001.
- [25] M. Franceschetti, O. Dousse, D. N. C. Tse, and P. Thiran, "Closing the gap in the capacity of wireless networks via percolation theory," *IEEE Transactions on Information Theory*, vol. 53, no. 3, pp. 1009–1018.
- [26] S. Guha, C.-K. Chau, and P. Basu, "Green wave: Latency and capacity-efficient sleep scheduling for wireless networks," in *Proc. of INFOCOM*, San Diego, CA, 2010.